Identification of Structural and Catalytic Classes of Highly Conserved Amino Acid Residues in Lysine 2,3-Aminomutase†

Dawei Chen,‡ Perry A. Frey,*,‡ Bryan W. Lepore,§ Dagmar Ringe,§ and Frank J. Ruzicka‡

Department of Biochemistry, University of Wisconsin, 1710 University Avenue, Madison, Wisconsin 53726, and Departments of Chemistry and Biochemistry, Program in Bioorganic Chemistry, and Rosenstiel Basic Medical Sciences Center, Brandeis University, 415 South Street, Waltham, Massachusetts 02254

Received June 30, 2006; Revised Manuscript Received August 16, 2006

ABSTRACT: Lysine 2,3-aminomutase (LAM) from *Clostridium subterminale* SB4 catalyzes the interconversion of (*S*)-lysine and (*S*)-*β*-lysine by a radical mechanism involving coenzymatic actions of *S*-adenosylmethionine (SAM), a [4Fe-4S] cluster, and pyridoxal 5′-phosphate (PLP). The enzyme contains a number of conserved acidic residues and a cysteine- and arginine-rich motif, which binds iron and sulfide in the [4Fe-4S] cluster. The results of activity and iron, sulfide, and PLP analysis of variants resulting from site-specific mutations of the conserved acidic residues and the arginine residues in the iron−sulfide binding motif indicate two classes of conserved residues of each type. Mutation of the conserved residues Arg134, Asp293, and Asp330 abolishes all enzymatic activity. On the basis of the X-ray crystal structure, these residues bind the *ϵ*-aminium and α-carboxylate groups of (*S*)-lysine. However, among these residues, only Asp293 appears to be important for stabilizing the [4Fe-4S] cluster. Members of a second group of conserved residues appear to stabilize the structure of LAM. Mutations of arginine 130, 135, and 136 and acidic residues Glu86, Asp165, Glu236, and Asp172 dramatically decrease iron and sulfide contents in the purified variants. Mutation of Asp96 significantly decreases iron and sulfide content. Arg130 or Asp172 variants display no detectable activity, whereas variants mutated at the other positions display low to very low activities. Structural roles are assigned to this latter class of conserved amino acids. In particular, a network of hydrogen bonded interactions of Arg130, Glu86, Arg135, and the main chain carbonyl groups of Cys132 and Leu55 appears to stabilize the [4Fe-4S] cluster.

Lysine 2,3-aminomutase (LAM)[1] catalyzes the interconversion of (*S*)-lysine and (*S*)-*β*-lysine, a reaction that proceeds by intramolecular migration of the α-amino group to the *β*-carbon with inversion of configuration and concomitant transfer of the 3-*pro-R* hydrogen in (*S*)-lysine to the 2-*pro-R* position of (*S*)-*β*-lysine (*1*, *2*). The enzyme contains a [4Fe-4S] cluster (*3*) and PLP and is activated by SAM. Hydrogen transfer is mediated by C5′ of the adenosyl moiety in SAM by a radical mechanism (*4*−*7*). Reversible reductive cleavage of SAM by the [4Fe-4S] cluster according to eq 1 generates the 5′-deoxyadenosyl radical (*8*, *9*), which in turn initiates the rearrangement reaction by the mechanism shown in Figure 1.

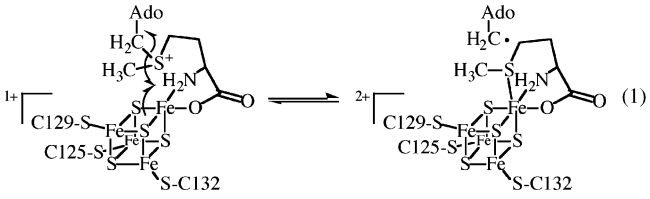

(1)

Abstraction of the 3-*pro-R* hydrogen from the lysyl side chain of the PLP-lysyl external aldimine by the 5′-deoxyadenosyl radical forms 5′-deoxyadenosine as a tightly bound intermediate. The resulting PLP-lysyl radical **1** undergoes isomerization by way of the azacyclopropylcarbinyl radical **2** to the product-related PLP-*β*-lysyl radical **3**. Abstraction of a hydrogen atom from the methyl group of 5′-deoxyadenosine by radical **3** forms the PLP-*β*-lysyl external aldimine and the 5′-deoxyadenosyl radical, completing the isomerization cycle (*10*, *11*).

PLP is bound to LAM as an internal aldimine with Lys337 (*12*, *13*). Reaction with (*S*)-lysine by transaldimination frees Lys337 and generates the external PLP-lysyl aldimine (Figure 1). A structure of the external aldimine shows the *ϵ*-aminium group of the lysyl side chain in hydrogen bonded contacts with Asp293 and Asp330 (*13*). Asp293 is highly conserved among species of LAM, and Asp330 is largely conserved but appears to be glutamate in a few species. The specificity of LAM for (*S*)-lysine may be determined by the interactions of Asp293 and Asp330 with the lysyl side chain.

LAM is a member of the radical SAM superfamily of enzymes that incorporate the generic CxxxCxxC sequence

† Supported by Grant DK28607 from the National Institute of Diabetes and Digestive and Kidney Diseases (P.A.F.) and Grant DBI 9874458 from the National Science Foundation (D.R.).

* To whom correspondence should be addressed: Department of Biochemistry, University of Wisconsin, 1710 University Ave., Madison, WI 53726. Telephone: (608) 262-0055. Fax: (608) 265-2904. E-mail: frey@biochem.wisc.edu.

‡ University of Wisconsin.

§ Brandeis University.

[1] Abbreviations: LAM, lysine 2,3-aminomutase; SAM, *S*-adenosyl-L-methionine; *Se*SAM, *Se*-adenosyl-L-selenomethionine; PLP, pyridoxal 5′-phosphate; IPTG, isopropyl thiogalactoside; DTT, dithiothreitol; PITC, phenyl isothiocyanate; EPPS, 4-(2-hydroxyethyl)-1-piperazinepropanesulfonic acid; PCR, polymerase chain reaction; WT, wild type.

10.1021/bi061329l CCC: $33.50
Published on Web 09/29/2006

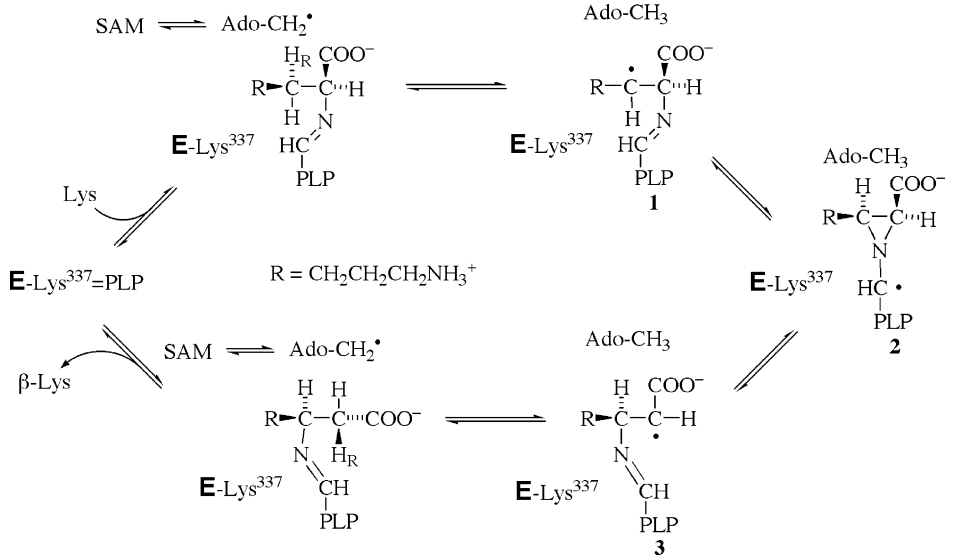

FIGURE 1: Mechanism of hydrogen transfer and isomerization in the action of LAM. The internal aldimine of PLP with Lys337 undergoes transaldimination with (*S*)-lysine to form the external aldimine between PLP and (*S*)-lysine. Reversible reductive cleavage of SAM generates the 5-deoxyadenosyl radical, which abstracts C3(H_R) from the lysyl side chain to form 5-deoxyadenosine and radical intermediate **1**, which then undergoes isomerization through the azacyclopropylcarbinyl radical **2** to form the product-related radical **3**. The product-related external aldimine of β-(*S*)-lysine with PLP arises through transfer of a hydrogen from the methyl group of 5′-deoxyadenosine to radical **3** into the C2(H_R) position, and transaldimination with Lys337 releases β-(*S*)-lysine.

as the basic binding motif for iron and sulfide in [4Fe-4S] centers (*14*). In LAM, the amino acid sequence of the iron and sulfide binding site is $_{125}$**C**SMY**C**RH**C**TRRR$_{136}$; the motif includes the absolutely conserved Arg130 and is flanked by three downstream arginine residues, two of which are conserved in homologous proteins found in the bacterial genome databases (*15*). The significance of these arginine residues is of interest. In this paper, we report the properties of specifically mutated variants of LAM, in which conserved arginine residues in the iron−sulfur motif are mutated, and of variants in which conserved acidic amino acids are mutated. The results are correlated with the structure of LAM in complex with (*S*)-α-lysine, PLP, and *Se*SAM (*13*).

MATERIALS AND METHODS

Coenzymes and Chemicals. Difco Terrific Broth, (*S*)-lysine monohydrochloride, $FeSO_4$, ampicillin, and tetracycline were obtained from Fisher. SAM, PLP, β-mercaptoethanol, DTT, and streptomycin sulfate were from Sigma. A standard iron solution was from Aldrich. PITC was from Pierce Chemical Co. Imidazole Ultrol Grade was from Calbiochem. Sephacryl S-200 HR, phenyl-Sepharose 6 Fast Flow High Substitution, and Q-Sepharose Fast Flow were from Amersham Biosciences. The pET23a(+) vector and Ni−NTA His Bind Resin were from Novagen. Pfu DNA polymerase, the QuikChange site-directed mutagenesis kit, and *Escherichia coli Epicurian coli* XL2-Blue MRF′ supercompetent cells were from Stratagene. *Nde*I and *Xho*I restriction endonucleases were Promega. The Zero Blunt TOPO PCR cloning kit was from Invitrogen. Centricon YM10 was from Millipore. (*S*)-[^{14}C]Lysine was from NEN Life Sciences. SAM was purified by chromatograpy through a 2 cm × 20 cm column of CM-cellulose eluted with 20 mM H_2SO_4 and was stored at −70 °C. Oligonucleotide primers for cloning and site-directed mutagenesis were obtained from the DNA Synthesis and Sequencing Laboratory, Biotechnology Center, University of Wisconsin.

Expression of LAM. The original expression system has *kamA* from *Clostridium subterminale* inserted into pET23a-(+) to give pAF-8/*kamA*. The latter is transformed into *E. coli* BL21(DE3) cells containing palter-Ex2/*argU*, expressing tRNA for rare codons AGA and AGG (*15*). Expression of *kamA* is enhanced by coexpression of *argU* (*15*). To facilitate purification, a vector expressing His-tagged LAM (C-terminus) was prepared from the original construct by removing the stop codon. Included in pET23a(+) is a series of six codons encoding hexahistidine after the multiple cloning site. Removing the stop codon for *kamA* allows expression of the hexahistidine tag. The pUC19 vector, E138 (*15*), containing the entire gene *kamA* from the genomic library was used as a template. The following PCR primers for pET23a(+), including *Nde*I and *Xho*I restriction sites and excluding the stop codon, were used: plus strand, 5′-TACACATATGATAAATAGAAGATATG; and minus strand, 5′-TAGACTCGAGTTCTTGAACGTGTCTC. PCR was conducted using Pfu DNA polymerase. The resulting blunt-ended oligonucleotide was ligated to the pCR BluntII TOPO vector. Digestion with *Nde*I and *Xho*I and purification by 2% agarose electrophoresis resulted in a 1.2 kb fragment ligated to pET23a(+) similarly cut with *Nde*I and *Xho*I and dephosphorylated. After transformation into *E. coli* XL2-Blue MRF′ competent cells, purified plasmid DNA was sequenced to verify the construct and used to transform *E. coli* BL21(DE3)/p-Alter-Ex2 *argU* cells.

Site-Directed Mutagenesis. Site-directed mutagenesis was conducted using the PCR-based QuikChange site-directed mutagenesis kit (Stratagene). Primers used for plus strands are listed in Table 1, and complementary primers were the minus strands. For PCR, 5−10 ng of template [pET23a(+)/*kamA* WT or pET23a(+)/*kamA* WT His-tag] and 125 ng of each primer were used. Mutated vectors were initially transformed into *E. coli* XL1 Blue competent cells. Plasmids obtained from colonies were sequenced in their entirety and used to transform *E. coli* BL21(DE3)/pAlter-Ex2/*argU* cells.

Table 1: Plus Strand Primers Used in Site-Directed Mutagenesis

mutation	plus strand primer
R130Q	5′-TGTGCTCAATGTACTGCCAACACTGTACAAGAAGAAGATTTGC
R134Q	5′-GTACTGCAGACACTGTACACAAAGAAGATTTGCAGGACAAAGCG
R135Q	5′-GTACTGCAGACACTGTACAAGACAAAGATTTGCAGGACAAAGCG
R136Q	5′-GTACTGCAGACACTGTACAAGAAGACAATTTGCAGGACAAAGCG
R130K	5′-TGTGCTCAATGTACTGCAAACACTGTACAAGAAGAAGATTTGC
R134K	5′-GTACTGCAGACACTGTACAAAAAGAAGATTTGCAGGACAAAGCG
R135K	5′-GTACTGCAGACACTGTACAAGAAAAAGATTTGCAGGACAAAGCG
R136K	5′-GTACTGCAGACACTGTACAAGAAGAAAATTTGCAGGACAAAGCG
E86Q	5′-CAAGCTATTCCAACAGCATTACAGCTTAACAAAGCTGCTGC-3′
D96N	5′-GCTGCTGCAGATCTTGAAAACCCATTACATGAAGATACAG-3′
D165N	5′-GAAATACTCCTCAAGTTAGAAACGTATTATTATCAGGTGGAG-3′
D172N	5′-CGTATTATTATCAGGTGGAAACGCTCTTTTAGTATCTG-3′
E236Q	5′-CTCACTTTAACCATCCAAATCAAATAACAGAAGAATCAACTAG-3′
D293N	5′-CCTTACTACATCTATCAATGTAACTTATCATTAGGACTTGAGC-3′
D330A	5′-GCGTACCAACATTCGTTGTTGCCGCTCCAGGTGGTGGTGG-3′
D330N	5′-GCGTACCAACATTCGTTGTTAACGCTCCAGGTGGTGGTGG-3′

Expression of Mutated LAM. Cells were cultured in Terrific Broth containing 100 μg/mL ampicillin and 10 μg/mL tetracycline and supplemented with 50 μM $FeCl_3$, 50 μM $ZnSO_4$, and 1 mM IPTG. Shake flasks (2 L) containing 1.5 L of medium were innoculated with a 6 h culture of each *E. coli* cell line. Cells were cultured for approximately 24−30 h at 37 °C with slow shaking (50−75 rpm) to minimize exposure to oxygen. Following the cell cultures, cells were harvested by centrifugation; cell pellets were frozen in liquid nitrogen and stored at −70 °C.

Purification of Wild-Type and Mutated LAM. All purification procedures were performed inside an anaerobic chamber (Coy, Grass Lake, MI). Wild-type LAM and R130Q-, R134Q-, R135Q-, and R136Q-LAM were expressed and purified without His tags as described previously (*15*). Protein yields from 30 g of cells were as follows: 500 mg for the wild type, 25 mg for R130Q-LAM, 375 mg for R134Q-LAM, 45 mg for R135Q-LAM, and 100 mg for R136Q-LAM.

His-tagged wild-type and mutated LAM were purified in the anaerobic chamber as follows. Approximately 30−40 g of frozen cells was added to 200 mL of lysis buffer [consisting of 50 mM KP_i (pH 8.0), 300 mM KCl, 0.1 mM (*S*)-lysine, 10 μM PLP, 2 mM β-mercaptoethanol, and 10 mM imidazole]. Cells were sonicated with six 30 s bursts (Fisher model 550 sonic dismembrator) at a setting of 8, keeping the temperature between 4 amd 8 °C. After being sonicated, cells were centrifuged at 100000*g* for 30 min at 4 °C. Supernatant fluids were applied directly to Ni−NTA His-Bind columns (4−5 cm × 2−2.5 cm) previously equilibrated with lysis buffer. After being washed with 200 mL of lysis buffer, the proteins were eluted with lysis buffer containing 175 mM imidazole. Imidazole eluates were passed through a Sephacryl-S200 column (5 cm × 30 cm) equilibrated with standard buffer [SB is 30 mM K-EPPS (pH 8.0), 20 μM $FeSO_4$, 10 μM PLP, 0.1 mM (*S*)-lysine, and 1 mM EPPS]. Pooled fractions were concentrated using Centricon YM10 spin columns to approximately 20−30 mg/mL prior to freezing and storage in liquid nitrogen. R136K-LAM was not produced from the mutated gene and could not be purified. Typical His-tagged protein yields from 30 g of cells were as follows: 400 mg for the wild type, 150 mg for R130K-LAM, 290 mg for R134K-LAM, and 90 mg for R135K-LAM.

Assays. LAM activity was assayed inside the anaerobic chamber as described previously (*6*). LAM was analyzed for iron, inorganic sulfide, and PLP by published methods (*16*−*18*).

The concentration of purified wild-type LAM was determined spectrophotometrically, using an ϵ_{280} value of 3.6×10^5 M^{-1} cm^{-1} (*19*), and correlated to the BCA protein assay (Pierce Chemical). Concentrations of mutated LAM could not be accurately measured by absorbance at 280 nm using the extinction coefficient for the wild-type enzyme because many mutations led to variations in the content of [4Fe-4S] clusters, which contribute to the absorption at 280 nm. Instead, the concentrations of mutated LAM were measured by use of the BCA protein assay (Pierce Chemical Co.) and correlated with a standard solution of wild-type LAM, the concentration of which had been determined by amino acid analysis as follows. Samples of purified *C. subterminale* SB4 LAM and the iron−sulfur reconstituted LAM were subjected to complete hydrolysis in 6 N HCl at 110 °C. Protein (5 μL, 100−125 μg) was added to hydrolysis tubes (Pierce Chemical Co., Rockford, IL) containing 700 μL of 6 N HCl. To half of the tubes was added 25 μL of an amino acid standard solution (each amino acid at 2.5 mM; Pierce Chemical Co.) in addition to the protein. Tubes were sealed in vacuo and heated for 24, 48, and 72 h at 110 °C. Following hydrolysis, samples were transferred to 2 mL microcentrifuge tubes and concentrated to dryness by vacuum centrifugation. The dried samples and amino acid standards were derivatized with PITC and separated by HPLC as described previously (*20*). Dried samples were dissolved in 100 μL of coupling buffer, concentrated to dryness by vacuum centrifugation, redissolved in 100 μL of coupling buffer and 10 μL of PITC, allowed to react for 30 min at room temperature, concentrated to dryness as described above, and dissolved in 1 mL of water prior to injection and separation by HPLC using a Beckman Gold HPLC system. The PITC derivative of each amino acid was separated by HPLC using a C18 reverse phase column (Phenomenex Gemini 5 μm, 4.6 mm × 25 cm, G-4435-EO), at a flow rate of 1 mL/min and room temperature with a sample injection volume of 50 μL. The eluting compounds were detected by spectrophotometry at a wavelength of 254 nm. The amino acids were resolved with a complex linear gradient composed of buffer A (0.05 M ammonium acetate in water) and buffer B (0.10 M

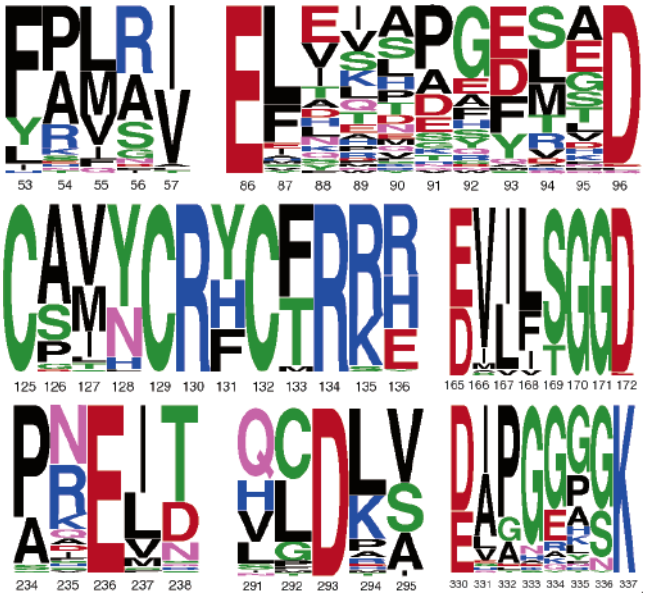

FIGURE 2: Key amino acid residues in highly conserved segments of LAM. The full lengths of 55 LAM sequences were aligned using progressive alignment with the Gonnet PAM 250 protein matrix weights (*22*) as implemented in Clustal_X and Clustal_W (*23*). The amino acids are depicted in standard letter codes, and the numbering corresponds to the sequence of LAM from *C. subterminale* SB4. The figure emphasizes the residues under consideration in highly conserved segments of the LAM sequence, as illustrated in logo format (*24*, *25*). Letters for fully conserved residues span the entire vertical space: examples include cysteine 125, 129, and 132 in the iron−sulfur motif characteristic of radical SAM enzymes. Letters for partially conserved residues share vertical space with other residues in proportion to the frequencies with which each appears in the 55 sequences. Thus, arginine appears most frequently at position 135, with lysine appearing less frequently.

ammonium acetate in 44% water, 46% acetonitrile, and 10% methanol). The gradient established was 0% buffer B for 5 min, 0 to 10% buffer B for 40 min, 10 to 35% buffer B for 35 min, 35 to 55% buffer B for 35 min, and 55 to 100% buffer B for 10 min. The PITC derivatives of each amino acid were eluted at the following retention times in minutes: Asx, 13; Glx, 18; Ser, 36; Gly, 39; His, 54; Thr, 56; Ala, 58; Arg, 60; Pro, 62; Tyr, 84; Val, 85; Met, 89; Ile, 98; Leu, 99; Phe, 108; and Lys, 117.

Reconstitution of [4Fe−4S] Clusters. Reconstitution of wild-type and mutated lysine 2,3-aminomutase was conducted anaerobically by the method of Hewitson et al. (*21*). To 200 μM (subunit) enzyme were added 1.2 mM $FeSO_4$, 1.2 mM Na_2S, and 5 mM dithiothreitol. The samples were incubated at room temperature for 4 h prior to gel filtration with a Sephacryl S200 HR column (2.5 cm × 25 cm) equilibrated with SB to separate excess reagent from protein. Protein fractions were collected and concentrated using Centricon YM10 spin columns (Amicon) to approximately 20−30 mg/mL prior to freezing and storage in liquid nitrogen.

RESULTS AND DISCUSSION

Conserved Amino Acid Residues in LAM. More than 50 genes in bacterial genomes have been annotated as encoding LAM. Figure 2 depicts the most highly conserved segments of amino acid sequences in 55 species of LAM, showing fully and highly conserved residues. Examples of fully

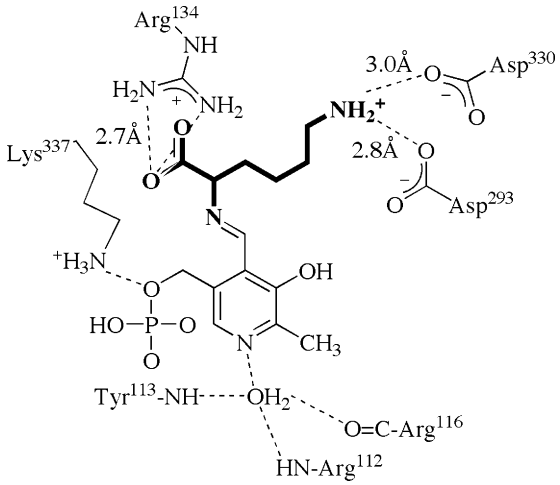

FIGURE 3: Hydrogen-bonded contacts of the lysyl-PLP external aldimine in the structure of LAM. The contacts shown are derived from the X-ray crystal structure of the complex of LAM with (*S*)-lysine, PLP, and *Se*SAM (*13*).

conserved residues include the cysteine 125, 129, and 132 in the iron and sulfide binding motif, as well as a number of acidic and basic residues. Some of the latter are engaged in binding the substrate or PLP. For example, the ϵ-amino group of conserved Lys337 binds PLP in the internal aldimine complex and is displaced by the α-amino group of the substrate lysine in the external aldimine complex depicted in Figure 3 (*12*, *13*). In contrast, Figure 2 shows that aspartate appears most frequently at position 330, as it does in *C. subterminale* LAM; however, glutamate appears at this position in *E. coli* LAM and a number of other species. In the following sections, we explore the functional roles of conserved acidic and basic amino acid residues in LAM from *C. subterminale*.

ϵ-Aminium Group of Lysine. The specificity of LAM for (*S*)-lysine as its substrate implies the existence of a binding locus for the ϵ-aminium group. In addition, the α-amino group engages in aldimine formation with PLP. Because the ϵ-aminium group is likely to be bound through an electrostatic interaction with an acidic residue of the enzyme, we mutated the conserved glutamate and aspartate residues and searched for a variant that lacked enzymatic activity but retained PLP, iron, and sulfide.

Purification of the wild-type and mutated LAM by the usual procedure, including hydrophobic and ion exchange chromatographic steps, routinely decreases the content of iron, sulfide, and PLP to amounts corresponding to fewer than one PLP and one [4Fe-4S] per subunit in the wild-type enzyme. The iron and sulfide can be restored by reconstitution, and PLP is added back in the standard assay.

In our initial experiments, however, we measured iron, sulfide, and PLP content without reconstitution to determine the consequences of mutation on the overall coenzyme content. Any mutation that weakened the binding of PLP and/or the [4Fe-4S] cluster would confer low activity for that reason irrespective of the binding of the substrate. Then, any variant lacking a specific glutamate or aspartate that contained substantial amounts of coenzymes but was entirely inactive could be considered to lack an essential acidic residue for binding the substrate.

The analytical results on mutations of conserved aspartate and glutamate residues are given in Table 2. The strictly

Table 2: Mutation of Conserved Glutamate and Aspartate Residues in His-Tagged LAM

	activity[a] (units/mg)	Fe/subunit[b]	S^{2-}/subunit[b]	PLP/subunit[b]
wild type	47 ± 6	2.7 ± 0.3	1.8 ± 0.2	0.70 ± 0.05
E86Q	8.5 ± 0.9	0.50 ± 0.02	0.40 ± 0.05	0.43 ± 0.03
D96N	0.08 ± 0.01	1.2 ± 0.1	0.95 ± 0.10	0.70 ± 0.05
D165N	0.04 ± 0.01	0.23 ± 0.01	0.13 ± 0.02	0.13 ± 0.02
E236Q	0.42 ± 0.03	0.70 ± 0.03	0.52 ± 0.03	0.17 ± 0.01
D172N	ND[c]	0.43 ± 0.02	0.13 ± 0.02	0.11 ± 0.02
D293N	ND[c]	0.97 ± 0.05	0.58 ± 0.03	0.23 ± 0.01
D330A	ND[c]	1.9 ± 0.1	1.3 ± 0.1	0.42 ± 0.07
D330N	ND[c]	1.0 ± 0.1	0.63 ± 0.05	0.60 ± 0.04

[a] Assayed by the radiochemical method as described previously (*6*). [b] Expressed as the number of ions or molecules per subunit as the mean value ± the standard deviation. [c] No detectable activity.

Table 3: Effects of Mutations of Arginine Residues on the Activity and Cofactor Content of LAM

	specific activity[a]	Fe/subunit	S^{2-}/subunit	PLP/subunit
WT	64 ± 5.2	3.2 ± 0.07	2.7 ± 0.06	0.97 ± 0.07
WT (FeS)[b]	88 ± 7.9	5.5 ± 0.19	4.9 ± 0.40	0.89 ± 0.04
WT (His)[c]	62 ± 1.7	2.9 ± 0.11	3.4 ± 0.08	0.66 ± 0.03
R130Q	<0.01	0.42 ± 0.01	0.20 ± 0.02	0.43 ± 0.03
R130K[c]	<0.01	0.20 ± 0.01	0.30 ± 0.02	0.84 ± 0.05
R130K (FeS)[b,c]	<0.01	3.0 ± 0.01	2.9 ± 0.10	0.82 ± 0.02
R134Q	<0.01	2.8 ± 0.05	2.7 ± 0.10	0.84 ± 0.03
R134K[c]	<0.01	1.5 ± 0.09	1.5 ± 0.05	0.59 ± 0.03
R135Q	0.98 ± 0.13	1.8 ± 0.02	1.5 ± 0.04	0.58 ± 0.02
R135K[c]	9.9 ± 0.68	2.4 ± 0.07	1.6 ± 0.01	0.77 ± 0.01
R136Q[d]	0.80 ± 0.01	0.48 ± 0.01	0.35 ± 0.02	0.98 ± 0.01
R136Q (FeS)[b]	0.85 ± 0.20	1.9 ± 0.02	1.6 ± 0.17	0.75 ± 0.02

[a] Specific activity (units per milligram of protein) assayed by derivatization of (*S*)-lysine and (*S*)-β-lysine as the PITC derivatives followed by HPLC separation, as described previously (*20*, *26*). [b] Iron−sulfur centers reconstituted. [c] His-tagged. [d] R136K, not expressed.

conserved residues did not include Asp330, which is glutamate in a few species, but the substitution of glutamate for aspartate can be considered conservative. The most striking observation is that all the mutations led to decreased iron and sulfide content in the purified variants and decreased PLP content in most of them. Activity could be detected in variants of Glu86, Asp96, Asp165, and Glu236, ruling them out as essential residues required for binding lysine. The acidic residues essential for activity include Asp172, Asp293, and Asp330. In the structure, the side chain carboxyl groups of Asp293 and Asp330 lie within hydrogen bonding distance of the ϵ-aminium group of the lysyl side chain in the external PLP aldimine, as illustrated in Figure 3 (*13*). Therefore, Asp293 and Asp330 not only interact with the lysyl ϵ-aminium group but also are essential for activity.

Mutations of Asp293 or Asp330, while they inactivate LAM, do not lead to such dramatic decreases in iron and sulfide content as mutation of Asp172 or most of the other conserved residues in Table 2. It seems that the other conserved acidic residues are more important for the structural integrity of LAM, and for the integrity of the [4Fe-4S] cluster, than either Asp293 or Asp330, each of which appears to facilitate the proper binding of lysine.

Conserved Arginine within and Adjacent to the Iron−Sulfur Motif. The aligned amino acid sequences of the known species of LAM show that Arg130 within the $_{125}$**C**SMY-**C**RH**C**TRRR$_{136}$ motif is conserved in all species, and Arg134 in the adjacent downstream cluster of arginine resides is also conserved in all species of LAM. Arginine 135 is present in 37 species, with lysine in its place in 13 other species. Arginine 136, present in 26 of 53 species, is least conserved, with glutamate or histidine often appearing in its place.

To examine the significance of the arginine residues, we mutated each of them, expressed and purified the variants, analyzed them for activity and iron, sulfide, and PLP content, and obtained the results given in Table 3. Mutation of Arg130 or Arg134 to either glutamine or lysine completely abolished enzymatic activity. Mutation of Arg130 also led to dramatically lower iron and sulfide content in the purified protein, although PLP binding was little affected. Mutation of Arg134 abolished activity without seriously decreasing the iron and sulfide content.

The importance of Arg130 to the integrity of the [4Fe-4S] cluster suggests a structural role for this residue. The structural graphic in Figure 4 depicts the likely contribution of Arg130 by showing how the side chain guanidinium moiety is within hydrogen bonding contact of the main chain carbonyl group of Leu55 and the γ-carboxylate of Glu86. The side chain of Arg130 seems, in effect, to cross-link the peptide chain between Arg130 and Leu55, while also constraining the chain at position 86 through a hydrogen-bonded electrostatic interaction with Glu86. Further, the main chain carbonyl of Arg130 is hydrogen bonded to the guanidinium group of Arg135, which is also hydrogen bonded to the main chain carbonyl group of Cys132 in the [4Fe-4S] cluster motif. Thus, the arginine claws of Arg130 and Arg135 seem to play important roles in maintaining the structural integrity required for stabilizing the iron−sulfur cluster.

Mutation of Arg134 to glutamine abolishes activity but only slightly decreases the iron, sulfide, and PLP content. Mutation to lysine abolishes activity and also substantially decreases the iron, sulfide, and PLP content. The structure shows that the carboxylate group of the lysyl-PLP external aldimine has a hydrogen-bonded ionic contact with Arg134 (*13*), and this is apparently essential for activity.

Mutations of Arg135 or Arg136 lead to low but significant activity. Mutation of Arg135 to glutamine significantly decreases the iron, sulfide, and PLP content, but this decrease is proportionally smaller than the loss of activity. Mutation of Arg135 to lysine is fairly well tolerated, with modest losses in activity and iron, sulfide, and PLP content. Mutation of Arg136 to glutamine leads to dramatically lower iron and sulfide content. Apparently, Arg135 is less important than the other arginine residues associated with the iron−sulfur cluster. Arginine 136 appears to be important in stabilizing the [4Fe-4S] cluster.

Reconstitution of Iron−Sulfur Clusters. The [4Fe-4S] clusters in LAM are not chemically stable, and chromatography of this protein during the course of purification tends to strip away iron and sulfide. Consequently, the purified enzyme never contains a full complement of iron−sulfur clusters, but they can be reconstituted by incubation of the enzyme with a reducing agent, ferrous sulfate, and sodium sulfide. Reconstitution increases the catalytic activity as well as the iron and sulfide content, as shown in the second row of Table 3. Reconstitution enhances the optical absorption band at 370 nm, as shown in Figure 5A. Reconstitution of R136Q-LAM also enhances this band and increases the iron

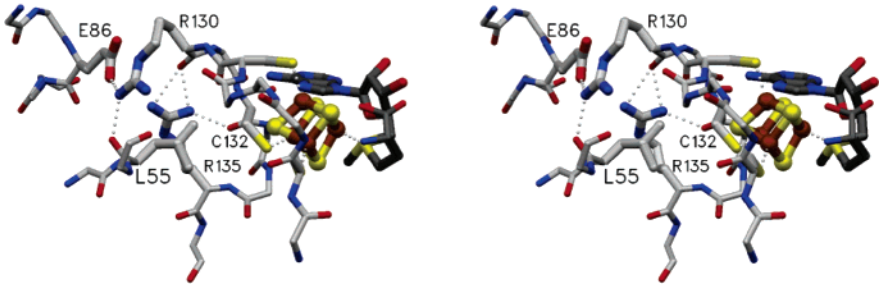

FIGURE 4: Roles of conserved arginine residues in stabilizing the fold of LAM. The hydrogen-bonded contacts of Arg130 and Arg135 are illustrated structurally in this model. Note how the guanidine group of Arg130 serves to cross-link three chain segments: the hydrogen bond to the main chain carbonyl group of Leu55 links the polypeptide chain between positions 55 and 130, and the hydrogen-bonded ionic interaction with Glu86 links the peptide chain between positions 86 and 130. The main chain carbonyl of Arg130 is in turn hydrogen bonded to the guanidinium group of Arg135. This figure was created in SETOR (*27*) by C. Kreinbring from PDB entry 2A5H (*13*).

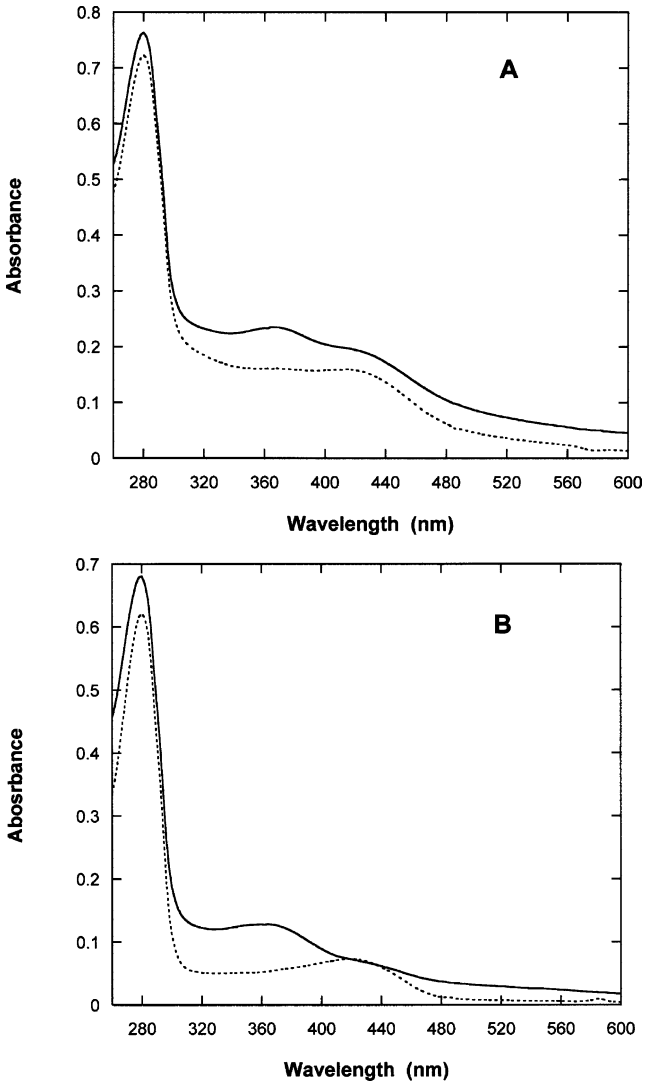

FIGURE 5: Spectral enhancement upon reconstitution of the iron−sulfur center in LAM. (A) Spectra of purified LAM before reconstitution (•••) and after reconstitution (—). (B) Spectra of purified R136Q-LAM before reconstitution (•••) and after reconstitution (—).

and sulfide content, as shown in Figure 5B and Table 3, but it does not increase the activity. Reconstitution of R130K-LAM also enhances the iron and sulfide content without increasing activity.

Correlation of Structure with Functional Amino Acids. As illustrated in Figure 6, the conserved arginine and acidic amino acid residues in LAM are located within the β-crescent fold at or peripheral to the active site. They fall into two functional categories, those that bind the ϵ-aminium and carboxylate groups of lysine at the active site and those that play significant roles in the structural integrity of LAM peripheral to the active site. The former includes Arg134, Asp293, and Asp330, which bind the lysyl carboxylate and ϵ-aminium groups. The functional importance of these groups is proven by the present mutagenic results, in which they are shown to be essential for activity, and the points of interaction are proven by the crystal structure (*13*). These residues do not seem to contribute decisively to the structural

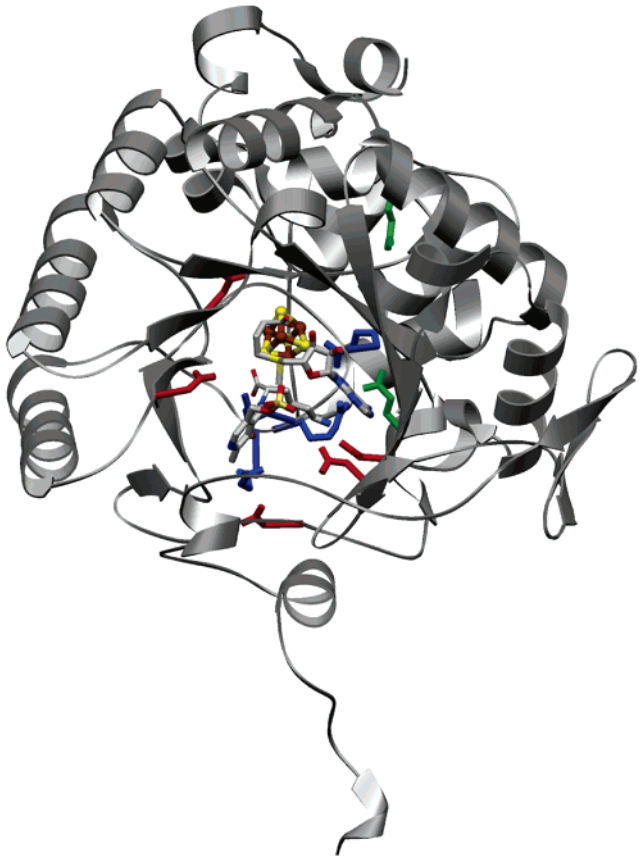

FIGURE 6: Locations of functionally important and conserved acidic and arginine residues in LAM. The structure of a LAM subunit is illustrated in a ribbon diagram showing the β-crescent (or open barrel) fold. The side chains of amino acid residues mutated in this work are shown as stick models: blue for arginine, red for aspartate, and green for glutamate. These residues appear either in the active site binding the substrate near the cofactors or peripheral to the active site but within the β-crescent. This figure was created in SETOR (*27*) by C. Kreinbring from PDB entry 2A5H (*13*).

integrity of LAM, as indicated by the fact that mutations do not result in major losses of iron, sulfide, or PLP in the purified enzyme.

In contrast, mutations of Arg130 and Asp172 completely abolish activity and destabilize the iron−sulfur centers. These residues are not in direct contact with the substrate or coenzymes and so must play a structural role, as further implied by the very low iron and sulfide contents of the purified variants. Mutations of Glu86, Asp96, Asp165, Glu236, and Arg136 lead to low but readily detectable activities in the variants, so these residues should not be regarded as being essential; however, mutations lead to moderate to severe destabilization of the iron−sulfur centers, indicating structural roles. An interaction network among Arg130 and Cys132 (main chain C═O), in the iron−sulfur motif, and Glu86, Arg135, and Leu55 (main chain C═O) shown in Figure 4 supports the assignment of structural roles to these residues.

The observation of instability in the iron−sulfur centers induced by a mutation is compatible with a structural role for that residue, but it does not prove that the loss in [4Fe-4S] clusters accounts for the decreased activity. Thus, reconstitutions of the iron−sulfur centers in R130K- and R136K-LAM do not restore activity (Table 3). Structural perturbations can lead to a myriad of consequences to activity and the binding of coenzymes and prosthetic groups.

REFERENCES

1. Chirpich, T. P., Zappia, V., Costilow, R. N., and Barker, H. A. (1970) Lysine 2,3-aminomutase. Purification and properties of a pyridoxal phosphate and *S*-adenosylmethionine-activated enzyme, *J. Biol. Chem. 245*, 1778−1789.
2. Aberhart, D. J., Gould, S. J., Lin, H.-J., Thiruvengadam, T. K., and Weiller, B. H. (1983) Stereochemistry of Lysine 2,3-Aminomutase Isolated from *Clostridium subterminale* Strain SB, *J. Am. Chem. Soc. 105*, 5461−5470.
3. Petrovich, R. M., Ruzicka, F. J., Reed, G. H., and Frey, P. A. (1992) Characterization of iron−sulfur clusters in lysine 2,3-aminomutase by electron paramagnetic resonance spectroscopy, *Biochemistry 31*, 10774−10781.
4. Moss, M., and Frey, P. A. (1987) The role of S-adenosylmethionine in the lysine 2,3-aminomutase reaction, *J. Biol. Chem. 262*, 14859−14862.
5. Baraniak, J., Moss, M. L., and Frey, P. A. (1989) Lysine 2,3-aminomutase. Support for a mechanism of hydrogen transfer involving S-adenosylmethionine, *J. Biol. Chem. 264*, 1357−1360.
6. Lieder, K. W., Booker, S., Ruzicka, F. J., Beinert, H., Reed, G. H., and Frey, P. A. (1998) *S*-Adenosylmethionine-dependent reduction of lysine 2,3-aminomutase and observation of the catalytically functional iron−sulfur centers by electron paramagnetic resonance, *Biochemistry 37*, 2578−2585.
7. Frey, P. A., and Magnusson, O. Th. (2003) S-Adenosylmethionine: A wolf in sheep's clothing, or a rich man's adenosylcobalamin? *Chem. Rev. 103*, 2129−2148.
8. Cosper, N. J., Booker, S. J., Ruzicka, F. J., Frey, P. A., and Scott, R. A. (2000) Direct FeS cluster involvement in generation of a radical in lysine 2,3-aminomutase, *Biochemistry 39*, 15668−15673.
9. Chen, D., Walsby, C., Hoffman, B. M., and Frey, P. A. (2003) Coordination and mechanism of reversible cleavage of S-adenosylmethionine by the [4Fe-4S] center in lysine 2,3-aminomutase, *J. Am. Chem. Soc. 125*, 11788−11789.
10. Frey, P. A. (1993) Lysine 2,3-aminomutase: Is adenosylmethionine a poor man's adenosylcobalamin? *FASEB J. 7*, 662−670.
11. Ballinger, M. D., Frey, P. A., Reed, G. H., and LoBrutto, R. (1995) Pulsed electron paramagnetic resonance studies of the lysine 2,3-aminomutase substrate radical: Evidence for participation of pyridoxal 5′-phosphate in a radical rearrangement, *Biochemistry 34*, 10086−10093.
12. Chen, D., and Frey, P. A. (2001) Identification of lysine 346 as a functionally important residue for pyridoxal 5′-phosphate binding and catalysis in lysine 2,3-aminomutase from *Bacillus subtilis*, *Biochemistry 40*, 596−602.
13. Lepore, B., Ruzicka, F. J., Frey, P. A., and Ringe, D. (2005) The X-ray crystal structure of lysine-2,3-aminomutase from *Clostridium subterminale*, *Proc. Natl. Acad. Sci. U.S.A. 102*, 13819−13824.
14. Sofia, H. J., Chen, G., Hetzler, B. G., Reyes-Spindola, J. F., and Miller, N. E. (2001) Radical SAM, a novel protein superfamily linking unresolved steps in familiar biosynthetic pathways with radical mechanisms: Functional characterization using new analysis and information visualization methods, *Nucleic Acids Res. 29*, 1097−1106.
15. Ruzicka, F. J., Lieder, K. W., and Frey, P. A. (2000) Lysine 2,3-aminomutase from *Clostridium* subterminale SB4: Mass spectral characterization of cyanogen bromide-treated peptides and cloning, sequencing, and expression of the gene kamA in *Escherichia coli*, *J. Bacteriol. 182*, 469−476.
16. Kennedy, M. C., Kent, T. A., Emptage, M., Merkle, H., Beinert, H., and Münck, E. (1984) Evidence for the formation of a linear [3Fe-4S] cluster in partially unfolded aconitase, *J. Biol. Chem. 259*, 14463−14471.
17. Wada, H., and Snell, E. E. (1961) The enzymatic oxidation of pyridoxine and pyridoxamine phosphates, *J. Biol. Chem. 236*, 2089−2095.
18. Beinert, H. (1983) Semi-micro methods for analysis of labile sulfide and of labile sulfide plus sulfane sulfur in unusually stable iron−sulfur proteins, *Anal. Biochem. 131*, 373−378.
19. Song, B. S., and Frey, P. A. (1991) Molecular Properties of Lysine 2,3-Aminomutase, *J. Biol. Chem. 266*, 7651−7655.
20. Heinrikson, R. L., and Meredith, S. C. (1984) Amino acid analysis by reverse-phase high-performance liquid chromatography: Precolumn derivatization with phenylisothiocyanate, *Anal. Biochem. 136*, 65−74.
21. Hewitson, K. S., Ollagnier-de Choudens, S., Sanakis, Y., Shaw, N. M., Baldwin, J. E., Munck, E., Roach, P. L., and Fontecave, M. (2002) The iron−sulfur center of biotin synthase: Site-directed mutants, *J. Biol. Inorg. Chem. 7*, 83−93.
22. Benner, S. A., Cohen, M. A., and Gonnet, G. H. (1994) Amino acid substitution during functionally constrained divergent evolution of protein sequences, *Protein Eng. 7*, 1323−1332.
23. Thompson, J. D., Gibson, T. J., Plewniak, F., Jeanmougin, F., and Higgins, D. G. (1997) The CLUSTAL_X windows interface: Flexible strategies for multiple sequence alignment aided by quality analysis tools, *Nucleic Acids Res. 25*, 4876−4882.
24. Crooks, G. E., Hon, G., Chandonia, J. M., and Brenner, S. E. (2004) WebLogo: A sequence logo generator, *Genome Res. 14*, 1188−1190.
25. Schneider, T. D., and Stephens, R. M. (1990) Sequence logos: A new way to display consensus sequences, *Nucleic Acids Res. 18*, 6097−6100.
26. Miller, J., Bandarian, V., Reed, G. H., and Frey, P. A. (2001) Inhibition of lysine 2,3-aminomutase by the alternative substrate 4-thialysine and characterization of the 4-thialysyl radical intermediate, *Arch. Biochem. Biophys. 387*, 281−288.
27. Evans, S. V. (1993) SETOR: Hardware lighted three-dimensional solid representations of macromolecules, *J. Mol. Graphics 11*, 134−138.

BI061329L